Available online at www.sciencedirect.com

SCIENCE DIRECT®

Polymer 46 (2005) 2365–2371

polymer

www.elsevier.com/locate/polymer

Studies on the reactive polyvinylidene fluoride-polyamide 6 interfaces: rheological properties and interfacial width

Yang Wu, Xiaobo Yu, Yuming Yang, Binyao Li, Yanchun Han*

State Key Laboratory of Polymer Physics and Chemistry, Changchun Institute of Applied Chemistry, Chinese Academy of Sciences, Changchun 130022, People's Republic of China

Received 13 January 2004; received in revised form 27 November 2004; accepted 18 January 2005

Abstract

We firstly synthesized and characterized a series of functional carboxylated polyvinylidene fluoride (PVDF-*g*-AAc). Then the temporal change of the complex viscosity (η^*) of the two plates consisting of the graft polymer PVDF-*g*-AAc and polyamide 6 (PA6) was measured by a rotational rheometer. There were two distinct stages for the change of the complex viscosity (η^*) with time: (i) stage I, where η^* increased rapidly at short times, a reaction-controlled kinetics was induced; (ii) stage II, where η^* increased slowly at a long time, however, a diffusion-controlled kinetics was obtained. Despite whether the kinetics are reaction-controlled or diffusion-controlled, the reaction could be predicted by pseudo-first-order kinetics. Meanwhile, the reaction temperature had an effect on the interfacial width and roughness. The value of the interfacial root-mean-square (rms) roughness obtained from AFM was consistent with that of the interfacial width from ellipsometer at different temperatures.

Keywords: Grafting functionalization; Rheology; Ellipsometer

1. Introduction

In order to improve a given polymer's properties, it is common to add another type of polymer to form a blend or alloy. However, in many cases, the so-obtained polymer mixture is immiscible and has poor mechanical properties. Two reasons are given for this. First, because the interfacial adhesion between the matrix phase and the dispersed phase is poor, external forces easily cause crazing between the phases. Second, as different domain sizes are formed during the mixing of the immiscible phases, the internal structure of the blend is not homogeneous. This causes uneven stress concentration to be generated in the blends, when mechanically deformed [1].

Therefore, the addition of block or graft copolymers has been widely attempted in order to solve such problems in blends [1–3]. These copolymers can be located at the interface between the immiscible polymers and play the role of emulsifiers. Owing to the resulting reduced interfacial tension, the dispersed domain sizes are found to decrease and its size distribution is more uniform. However, a problem with introducing a pre-made copolymer to the blend is that it is difficult for the copolymer to reach the interface so that in most cases an insufficient number of the copolymers are located at the interface to play the role of emulsifiers. Further, the copolymers can form micelles [4]. Thus, adding preformed copolymers is not always attractive. Recently, a procedure called 'reactive blending' has been developed, in which reactive sites incorporating both blend components form covalent bonds between them, resulting in the in situ formation of the copolymer at the interface during mixing of the blend components [1,5–7]. In this process, the copolymer is exactly located at the interface after melt blending. Moreover, the synthesis of the copolymer emulsifier can be omitted. Reactive blends are usually prepared by using an internal mixer or an extruder, where there is complex flow combined by shear and elongational flows. Thus, some research groups employ

---

* Corresponding author. Tel.: +86 431 526 2175; fax: + 86 431 526 2126.

E-mail address: ychan@ciac.jl.cn (Y. Han).

0032-3861/$ - see front matter © 2005 Elsevier Ltd. All rights reserved.
doi:10.1016/j.polymer.2005.01.048

a planar geometry of two polymers: for instance, two layers of each polymer are joined [8–15]. In this situation, the initial interface is well-defined and very sharp. Because the effect of complex external flow on interfacial morphology is excluded, the interface morphology depends mainly upon reaction conditions (time, temperature, and the amount of the reactive groups) as well as the viscoelastic properties of the two polymers.

Although this method is industrially more appealing, the characteristics and properties of the interface are not fully understood yet. In the past several years, fundamental approaches in theory and experiments have just started to be reported [16–20]. Fredrickson [16,17] and O'Shaughnessy et al. [18,19] independently reported the theoretical results on the kinetics of the coupling reaction held at the immiscible polymer–polymer interface. They proposed the three time regimes for the diffused-controlled coupling of end-functionalized A and B homopolymers at an A–B interface [17] and categorized the reaction depending on the reactivity of the functional groups and the stage of the reaction [18,19]. Oyama and Inoue [13,20] theoretically and experimentally studied the kinetics of the coupling between functionalized polymer chains at the immiscible polymer–polymer interface and demonstrated that the overall kinetics followed an apparent first-order behavior. Recently, Kim et al. [14] developed a rheological technique to evaluate the reaction kinetics of monocarboxylated polystyrene (PS-*m*COOH) and poly (methyl-methacrylate-*ran*-glycidyl methacrylate) (PMMA-GMA) by employing the assumption that the rheological properties were related to the amount of the in situ formed graft (or block) copolymers for a reactive blend. Thus, the reaction kinetics might be evaluated if one monitors temporal changes of rheological properties. This rheological method is, of course, much easier than more spectroscopic methods such as forward recoil spectrometry (FRES), neutron scattering and X-ray photoelectron spectroscopy (XPS). The technique does not require any labeling, even though the excess of interface is not determined quantitatively.

It is well known that PVDF has good weathering resistance, good chemical resistance and excellent barrier action. However, it is impact sensitive. PA6 has good mechanical properties, but it is not resistance to weathering and has poor barrier action. Combing the properties of the two polymers constitute, a high performance engineering polymer might be produced. Unfortunately, they are immiscible over whole composition range [21], which result in lower mechanical properties. Recently, the graft and modification of PVDF was extensively exploited [22, 23], among which grafting with acrylic acid is especially universal. Here we introduce the PVDF-*g*-AAc/PA6 blends to study the reactive interface.

A rheological technique to evaluate the reaction kinetics of a functional carboxylated PVDF (PVDF-*g*-AAc) and polyamide 6 (PA6) is introduced. The reaction between the carboxylic acid in PVDF-*g*-AAc and the amine groups in PA6 occurs at higher temperatures, giving the in situ graft copolymers of PVDF-*g*-AAc-*g*-PA6. The interface width with reaction time is studied by ellipsometer and interface roughness by AFM after selectively removing the unreacted top layers.

2. Experimental part

2.1. Materials and reagents

Polyamide 6 (PA6) (number-average molar mass is 2.4×10^4 g/mol) was supplied by Heilongjiang Nylon Plastic Factory. PVDF (mass average and number-average molar masses are 16.6×10^4 and 9.9×10^4 g/mol, respectively) used in this work was SOLEF 11010 from Solvay. The monomer acrylic acid (AAc) (purity above 99%), 1-methyl-2-pyrrolidone (NMP) and formic acid were obtained from Beijing Yili Fine Chemical Co. *N*,*N*-dimethylformamide (DMF) was from Beijing Chemical Plant.

2.2. Graft copolymerization of PVDF with acrylic acid: PVDF-*g*-AAc copolymer [22,23]

About 100 g of PVDF films were placed in polyethylene-lined paper envelopes and irradiated with a ^{60}Co to a total dose of 15 KGy. After irradiation, the polymer was found to be still completely soluble in DMF, indicating that no crosslinking took place under these conditions. The irradiated powder was conditioned at room temperature for 48 h in order to allow the formation of peroxy groups to take place from reactions with atmospheric oxygen before being stored in a refrigerator at −35 °C for subsequent use.

Ten grams irradiated PVDF was dissolved in 125 mL NMP. The PVDF solutions and AAc monomer were introduced into a three necked, round-bottom flask equipped with a thermometer, a condenser, and a gas line. The AAc monomer concentrations were 0.05, 0.15 and 0.30 g/mL, respectively. The final volume of reaction mixture was adjusted to 200 mL. The solution was saturated with purified nitrogen for 30 min under stirring. The reactor flask was then placed in a thermostated water bath at 60 °C to initiate the graft copolymerization reaction. A constant flow of nitrogen was maintained during the thermal graft copolymerization process. After 3 h, the reactor flask was cooled in a cool water bath, and the AAc graft copolymerized PVDF (PVDF-*g*-AAc) was precipitated in excess ethanol (a good solvent for the AAc homopolymer). After filtration, the PVDF-*g*-AAc copolymer was redissolved in 200 mL of acetone and then reprecipitated in 1000 mL of ethanol. The above procedure was repeated for another two times. The PVDF-*g*-AAc sample was further purified by stirring for 24 h in an excess amount of distilled water at 55 °C to remove the residual AAc homopolymer, if any. The graft concentration of acrylic acid was determined by chemical titration and FT-IR. FT-IR spectra of the thin copolymer films fabricated from compression-molding were obtained from a Bio-Rad FTS 135 FT-IR spectrophotometer.

2.3. Rheological properties

Two plates, one for PVDF-*g*-AAc (or neat PVDF) and the other for PA6, were prepared by compression molding on glass plate at 180 and 240 °C, respectively, and then annealed at 125 °C for 24 h. This method gave a very smooth surface of the polymer plates. The thickness of each plate was about 0.3 mm, and the diameter was 25 mm. As soon as two plates were put into a rheometer (Physica MCR300.) at 200 °C under a nitrogen environment, the complex viscosity (η^*) was monitored with time. Here, time zero was defined as the time when the heating chamber of the rheometer was closed. It is noted that the lower viscosity material (PVDF-*g*-AAc) was placed at the top. The strain amplitude (γ_0) and the angular frequency (ω) were 0.005 and 0.2 rad/s, respectively, which lies in the linear viscoelastic regime.

2.4. Interfacial measurement

In order to measure the interfacial width between these PVDF-*g*-AAc and PA6 specimens, bilayer films were prepared as follows. First, a PA6 substrate with ca. 0.5 mm thickness was prepared by compression molding at 240 °C between glass plates in order to obtain an optically flat surface. Meanwhile, a PVDF-*g*-AAc film of about 300 nm was prepared by spin-coating from a 5 wt % DMF solution onto a PA6 substrate. The bilayer specimen thus prepared was dried under vacuum at 50 °C for 24 h. The bilayer refractive index of PVDF-*g*-AAc ($n_{\text{PVDF-}g\text{-AAc}}$) was estimated as 1.44 at room temperature and that of PA6 (n_{PA6}) was 1.53 so that the present bilayer film fulfilled the requirement, $|n_{\text{PVDF-}g\text{-AAc}}\text{-}n_{\text{PA6}}| \geq 0.02$. The bilayer film was placed in a hot chamber of the ellipsometer (UVISEL P/N 23301916). The retardation, Δ, and reflection ratio, tan Ψ, of reflected light were measured directly, from which both the interfacial width (λ) and the thickness of the upper layer, PVDF-*g*-AAc, could be estimated using the pre-estimated values of $n_{\text{PVDF-}g\text{-AAc}}$ and n_{PA6} at the experimental temperature. The refractive index of the interphase was approximated to be uniform and equal to an average of the refractive index of each component polymer, $n = (n_{\text{PVDF}-\text{g}-\text{AAc}} + n_{\text{PA6}})/2$. The details of the ellipsometric analysis and the computation were as described in Ref. [24].

2.5. Atomic force microscope sample preparation

PVDF-*g*-AAc was dissolved in DMF (5 wt % PVDF-*g*-AAc) and then spun at 2000 rpm onto silicon wafers. After drying, a layer of 6 wt % PA6 from formic acid was spin-coated directly on the PVDF-*g*-AAc-coated wafers. The formic acid did not dissolve or significantly swell the AAc-*g*-PVDF film. After drying, these bilayer films were annealed at 150, 180 and 200 °C for 4 h in a vacuum to allow grafting to occur. Grafting is expected to occur by reaction of the amine end on the PA6 with a carboxylic acid group on the PVDF-*g*-AAc to form an amide bond.

The topography of the interface was examined by atomic force microscopy (AFM) after selectively washing away the ungrafted PA6 from the top surface of the PVDF-*g*-AAc layer. Bilayer of the grafting polymers were first prepared on a 1×1 cm^2 silicon wafer and annealed as described above. Samples were then washed in 50 mL of formic acid at room temperature for 24 h and dried in vacuum. An AFM (SPA300HV/SPI3800N) from Seiko Instruments with a pyramidal Si_3N_4 tip (nominal spring constant of 2 N m^{-1}) was used for all AFM measurements.

3. Results and discussion

3.1. Synthesis and characterization of the PVDF-g-AAc

Free radicals brought out on the PVDF chains during γ-ray irradiation, and it transferred into stable peroxides at room temperature. When it was conditioned in the solution at 60 °C with nitrogen atmosphere, the peroxides split into new free radicals, which reacted with AAc monomer rapidly and formed the graft copolymer PVDF-*g*-AAc. The FT-IR spectra of PVDF-*g*-AAc thin films with different graft concentrations are shown in Fig. 1. A characteristic band for the O–C–O stretching ($\nu = 1712$ cm^{-1}) associated with the COOH groups of the grafted AAc chains were found for all PVDF-*g*-AAc films. It confirmed that AAc was grafted on to PVDF.

The graft concentration of the acrylic acid onto PVDF was determined by chemical titration. It showed that the graft concentration increased with the increase of [AAc] to [PVDF] feed ratio for the graft copolymerization, i.e. the

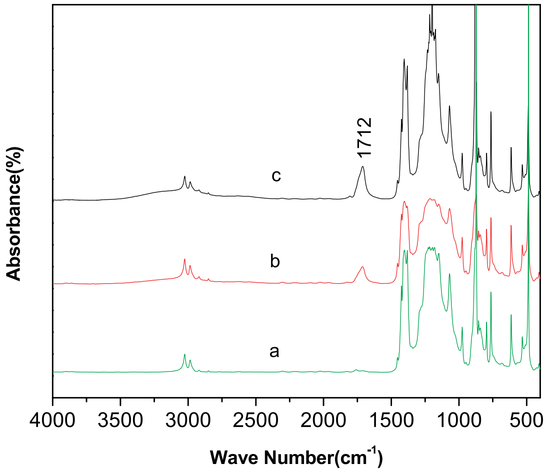

Fig. 1. FTIR spectra of samples with different [AAc] to [PVDF] feed ratio: (a) [AAc]/[PVDF] = 1; (b) [AAc]/[PVDF] = 3; (c) [AAc]/[PVDF] = 6.

graft concentration was 0.36, 2.88 and 6.84 wt% for [AAc] to [PVDF] feed ratio of 1, 3 and 6, respectively.

3.2. Rheological properties

PVDF-*g*-AAc with the graft concentration of G_{AAc} wt% = 6.84% is selected to blend with PA6 in the following study. The plots of complex viscosity (η^*) with time at 200 °C for PVDF/PA6 and PVDF-*g*-AAc/PA6 blends are shown in Fig. 2. For a blend of PVDF and PA6, there is a small Flory's interaction parameter. As the welding time (or contact time in the rheometer) goes on, the two polymer chains interdiffuse and the interface is thickened, then a final interfacial width of about 5 nm is obtained, which causes η^* to increase slowly with the welding time and reaches a steady value at a considerably long time (about 170 min). After that, η^* does not change any more [14].

For a reactive blend consisting of PVDF-*g*-AAc and PA6, η^* increases rapidly within short times (about 30 min). Then η^* increases slowly to reach a steady value till about 600 min. This phenomenon is quite different from the nonreactive PVDF/PA6 blend. For a reactive blend, the graft (or block) copolymer forms at the interface by the in situ coupling reactions, which improve the interfacial adhesion strength. Then, η^* must increase accordingly. Thus, the rheological properties (η^*) are related to the amount of the in situ formed graft copolymers (Σ) for a reactive blend. If we define Σ^* as the saturation areal density of copolymer at the interface and η^{**} as the equilibrium complex viscosity, ($\Sigma^* - \Sigma$) and ($\eta^{**} - \eta - \eta^*$) can be considered as the residual amount necessary to reach the saturation areal density of the copolymer and the potential complex viscosity available for the increase, respectively. In this case, relation between ($\Sigma^* - \Sigma$) and (η^{**}-η^*) is linear, i.e. $(\Sigma^* - \Sigma) \propto (\eta^{**}\text{-}\eta^*)$. According to Oyama's and Inoue's works [13,20]: when the supply of both reactive groups is sufficient at the interface in the reaction time scale, the reaction rate, r_{AB}, would vary proportionally to the vacant sites available for the reaction, resulting in the pseudo-first-order kinetics in ($\Sigma^* - \Sigma$), as shown by the next kinetic equations

$$r_{AB} = k_{AB}(C_A - C_{AB})(C_B - C_{AB})(\Sigma^* - \Sigma) \tag{1}$$

$$r_{AB} = k_{AB}C_A C_B(\Sigma^* - \Sigma) \quad (C_A, C_B \gg C_{AB}) \tag{2}$$

Where k_{AB} is the rate constant, C_{AB} is the concentration of the copolymers formed at time t, and C_A and C_B are the concentration of A and B reactive groups prior to the reaction, respectively. The equation also indicates the time dependence of $\Sigma \sim -\exp(-t)$.

In our case, the reaction kinetics is examined by carrying out the second-order (Fig. 3) analyses, that is, plot $1/(\eta^{**}$-$\eta^*)$ vs. time, based on the assumption that the reaction rate would vary with $(\Sigma^* - \Sigma)$ and the relation $(\Sigma^* - \Sigma) \propto (\eta^{**} - \eta^*)$.

On the basis of the results given in Fig. 2, η^* of the reactive blend is divided into two different stages: stage I, η^* increases rapidly with reaction time at short times; stage II, where η^* increases slowly at long time before reaching a steady value.

Stage I. Because the interface adhesion strength increases due to the coupling reaction between carboxylic acid and amine groups with the reaction time, η^* increases rapidly. During this stage, most of the reaction occurs between the reactive groups existing at the interfacial region. Therefore, the process is controlled by the reaction between the reactive groups.

Stage II. An incubation period was not found where η^* did not increase with time as Kim reported [14]. It might be due to the lower reactivity between the carboxylic acid and amine groups in our case than that between the mono-carboxylate and glycidyl methacrylate (GMA) groups. The interface is not totally occupied by the in situ formed graft copolymer. At the initial time in the stage, the reactive chains in the interfacial region are completely consumed, so there is a depletion hole of reactive groups in the interfacial region. Therefore, more reactive groups in the bulk will diffuse into the interfacial region as the lower reactive group concentration there so that the additional reactions can

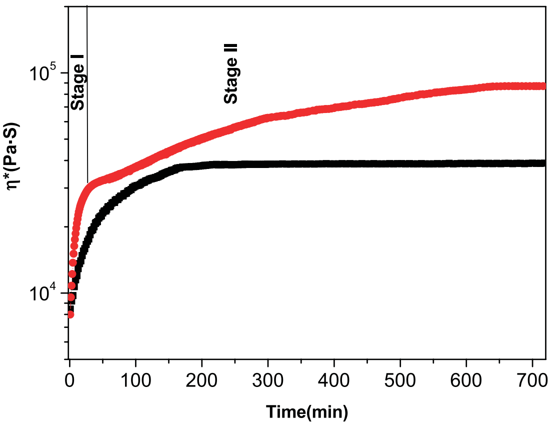

Fig. 2. Plots of η^* vs. time for PVDF-*g*-AAc /PA6 (●) and PVDF/PA6 (■) at 200 °C.

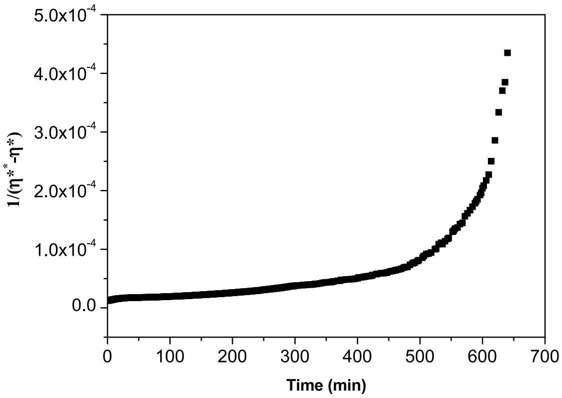

Fig. 3. Plot of $1/(\eta^{**} - \eta^*)$ vs. time for PVDF-*g*-AAc /PA6 at 200 °C.

proceed. At the same time, the in situ formed graft copolymers can split out due to their lower reactivity or escape from the interface due to the thermal fluctuation, which keep to a dynamic equilibrium. It causes the complex viscosity increases slowly.

We can conclude from the above results that the difference in the reaction rate during stage I and II might be due to the fact that reaction in the interfacial region controls the amount of the graft copolymer during stage I, whereas the diffusion of reactive groups becomes dominant during stage II.

Pseudo-first-order kinetics applies when the spatial restriction at the interface or unavailability of one of the reactive groups terminates the reaction [20]. In our case, the content of the carboxylate groups is larger than that of amine groups. Then, the shortage of amine group terminates the reaction. Fig. 3 testified that the coupling reaction was consistent with the pseudo-first-order kinetics in the whole stage. That is, the amount of the vacant sites available for further reaction at the interface scales with the reactive time. Despite whether the kinetics are reaction-controlled or diffusion-controlled, the reaction could be predicted by the pseudo-first-order kinetics.

3.3. Interfacial width and roughness

The interfacial width, λ, between PVDF-*g*-AAc and PA6 was measured by ellipsometer. Fig. 4 shows the time dependence of the interfacial width of PVDF-*g*-AAc /PA6 at three different reaction temperatures. The reaction temperature has a significantly effect on the interfacial width. The interfacial width increased drastically above the melting point of PVDF (about 170 °C). It was only 12 nm at 150 °C and reached 31 nm at 180 °C and 37 nm at 200 °C. Here, the restriction of the chain mobility of both PVDF and PA6 under 170 °C resulted in a thin interface. Thus, it is essential for at least one of the phases to possess molecular chain mobility in order for the functional groups to encounter efficiently to form covalent bonds between them, resulting in a thick interface.

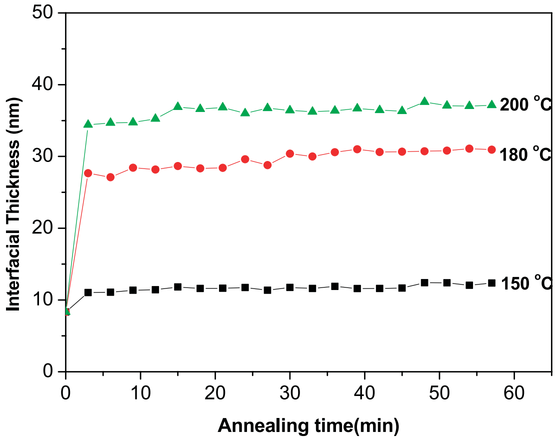

Fig. 4. Annealing time dependence of the interfacial thickness, λ, of the PVDF-*g*-AAc /PA6 blend at different annealing temperatures.

Next, the observed interfacial width of about 37 nm was compared with the calculated dimension of the coil size as follows. It was assumed that the coil size of the copolymer was not seriously changed by the effects from the adjacent comonomer, such as steric hindrance or repulsive forces. Thus, the coil size of the copolymer formed at the interface could be roughly estimated from the following equation:

$$[\text{the coil size of the copolymer}] \approx 2\langle s^2\rangle^{1/2}_{\mathrm{PVDF}} + 2\langle s^2\rangle^{1/2}_{\mathrm{PA6}} \qquad (3)$$

where $\langle s^2\rangle^{1/2}$ is the root-mean-square radius of gyration of the component polymer. As the root-mean-square end-to-end distance, $\langle r^2\rangle^{1/2}_{\mathrm{PA6}} = 9.7\times10^{-2}\ \mathrm{M}^{1/2} = 15.0$ nm for PA6 [25], the $\langle s^2\rangle^{1/2}_{\mathrm{PA6}}$ was roughly estimated to be 6.1 nm from the relationship, $\langle s^2\rangle = \langle r^2\rangle/6$. Meanwhile, $\langle s^2\rangle^{1/2}_{\mathrm{PVDF}} = 3.3\times10^{-2}\ \mathrm{M}_w^{1/2} = 13.4$ nm for [25]. Then, the coil size of the copolymer calculated from the equation is 39.0 nm. In other words, the observed interfacial width of about 37 nm is almost as large as the coil size of the whole copolymer, which is far from almost twice as large as Koriyama reported [12]. This implies that the present reactive interface has a structure composed of two blend component polymers and copolymers formed between them, but there are no micelle or microemulsions formation due to their far lower reactivity.

As the formation of the graft copolymer, it must result in a decrease of the polymer/polymer interfacial tension. In according to Lyu's theory [11]: the decrease of the interfacial tension due to the creation of the block copolymers and the thermal fluctuation induced deformations at interfaces lead to a morphological changes. Therefore, the interfacial morphology after annealing for 4 h at different temperatures was observed (Fig. 5). The values of the root-mean-square (rms) roughness at 150, 180 and 200 °C are 9.4, 32, and 35 nm, respectively, which is consistent with the interfacial width at different temperatures. It further confirmed that the reactive interface was occupied by a layer of the in situ formed copolymer.

Why did an interfacial width reach equilibrium in a short time though the complex viscosity reached equilibrium in a long time for a reactive blend? Since the interfacial width (λ) was estimated by assuming the pre-estimated value of $n = (n_{\mathrm{PVDF}-g-\mathrm{AAc}} + n_{\mathrm{PA6}})/2$, ellipsometer could determine the interfacial width roughly. However, it could not measure the amount of the in situ formed copolymer accurately because within certain interfacial thickness, excessive copolymer did not nearly lead to any change of the value of $n = (n_{\mathrm{PVDF-g-AAc}} + n_{\mathrm{PA6}})/2$ while the amount of in situ formed copolymer reach a critical value. Thus, it was testified that an interfacial width reached equilibrium in a short time by ellipsometer. However, as described above, since the rheological properties are related to the amount of

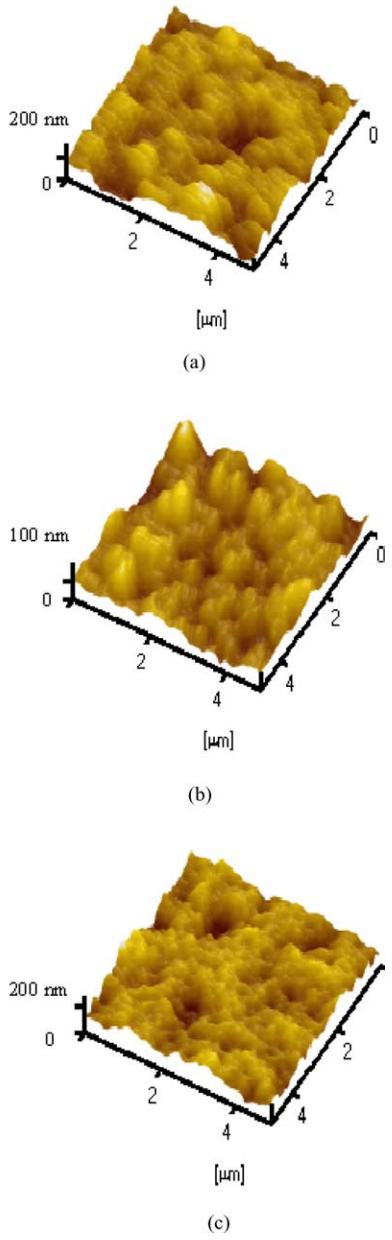

(a)

(b)

(c)

Fig. 5. AFM topographic images (5×5 µm) for the PVDF-*g*-AAc/PA6 blend reacted at different temperatures for 4 h: (a) $T=150$ °C; (b) $T=180$ °C; and (c) $T=200$ °C. The RMS roughness at the reaction temperatures of 150, 180 and 200 °C are 9.4, 32, and 35 nm, respectively.

the in situ formed graft (or block) copolymer for a reactive blend, η^* would continue to increase till the amount of the in situ formed copolymer reach the saturation areal density of copolymer. It would take a long time to achieve, so that complex viscosity reached equilibrium in a long time, which is consistent to the rheological results.

4. Conclusions

A series of functional carboxylated polyvinylidene fluoride (PVDF-*g*-AAc) was synthesized and characterized by FT-IR. Chemical titrations showed that the graft concentration increased with the increase in [AAc] to [PVDF] feed ratio. Rheological method was employed to observe the reaction kinetics in the reactive blending system. Two distinct stages can be considered for the reactive blends with planar geometry. In stage I, because of the increase of interfacial coupling reaction between carboxylic acid and amine groups, η^* increased rapidly with reaction time. In this stage, the growth mechanism is reaction-controlled kinetics. In stage II, η^* increased slowly because there were a dynamic equilibrium between the reactive groups diffusing into the interface and the in situ formed graft copolymer partly splitting out as their lower reactivity or leaving the interface as the thermal fluctuation. The growth mechanism is a diffusion-controlled kinetics. Despite whether the kinetics are reaction-controlled or diffusion-controlled, the reaction could be predicted by pseudo-first-order kinetics.

Meanwhile, according to the interfacial width changes measured by ellipsometer and the interfacial morphological changes measured by AFM, it is found that the reaction temperature has an effect on the interfacial width and roughness. The value of the interfacial root-mean-square (rms) roughness obtained from AFM was consistent with that of the interfacial width from ellipsometer at different temperatures.

Acknowledgements

This work is subsidized by the National Natural Science Foundation of China (50125311, 20334010, 20274050, 50390090, 50373041, 20490220, 20474065, 50403007), the Ministry of Science and Technology of China (2003CB615601), the Chinese Academy of Sciences (Distinguished Talents Program, KJCX2-SW-H07), and the Jilin Distinguished Young Scholars Program (20010101).

References

[1] Utracki LA. Polymer alloys and blends. Munich: Hanser; 1989.
[2] Gersappe D, Irrine D, Balazs AC, Liu Y, Sokolov J, Rafailovich M, Schavarz S, Peiffer DG. Science 1994;265:1072.
[3] Macosko CW, Guégan P, Khandpur AK, Inoue T. Macromolecules 1996;29:5590.
[4] Dai HK, Kramer EJ, Shull KR. Macromolecules 1992;25:220.
[5] Yin Z, Koulic C, Pagnoulle C, Jérôe R. Macromolecules 2001;34:5132.
[6] Shi DA, Ke Z, Yang J, Gao Y, Wu J, Yin JH. Macromolecules 2002;35:8005.
[7] Pernot H, Baumert M, Count F, Leibler L. Nat Mater 2003;1:54.
[8] Schulze JS, Moon B, Lodge TP, Macosko CW. Macromolecules 2001;34:200.
[9] Schulze JS, Cernohous JJ, Hirao A, Lodge TP, Macosko CW. Macromolecules 2000;33:1191.

[10] (a) Jiao J, Kramer EJ, de Vos S, Möller M, Koning C. Polymer 1999; 40:3585.
(b) Jiao J, Kramer EJ, de Vos S, Möller M, Koning C. Macromolecules 1999;32:6261.

[11] Lyu SP, Cernohous JJ, Bates FS, Macosko CW. Macromolecules 1999;32:106.

[12] Koriyama H, Oyama HT, Ougizawa T, Inoue T, Weber M, Koch E. Polymer 1999;40:6381.

[13] Oyama HT, Ougizawa T, Inoue T, Weber M, Tamaru K. Macromolcules 2001;34:7017.

[14] Kim JY, Jeong U, Kim JK. Macromolecules 2003;36:1594.

[15] Yin Z, Koulic C, Pagnoulle C, Jérôe R. Langmuir 2003;19:453.

[16] Fridrickson GH. Phys Rev Lett 1996;76:3440.

[17] Fredrickson GH, Milner ST. Macromolecules 1996;29:7386.

[18] O'Shaughnessy B, Sawhney U. Phys Rev Lett 1996;76:3444.

[19] O'Shaughnessy B, Sawhney U. Macromolecules 1996;29:7230.

[20] Oyama HT, Inoue T. Macromolecules 2001;34:3331.

[21] Liu ZH, Maréchal Ph, Jérôme R. Polymer 1998;39:1779.

[22] Mascia L, Hashim K. Polymer 1998;39:369.

[23] Yang L, Wang P, Kang ET, Neoh KG. Macromolecules 2002;35:673.

[24] Yukioka S, Nagato K, Inoue T. Polymer 1993;33:1171.

[25] Brandrup J, Immergut EH, editors. Polymer handbook. 4th ed. New York: Interscience; 1999.